Materials Science Forum
ISSN: 1662-9752, Vol. 925, pp 104-109
doi:10.4028/www.scientific.net/MSF.925.104

Submitted: 2017-10-04
Revised: 2018-03-12
Accepted: 2018-03-12
Online: 2018-06-20

X-Ray Imaging of Formation and Growth of Spheroidal Graphite in Ductile Cast Iron

H. Yasuda[1,a], A. Sugiyama[2], C. Kiattisaksri[1], K. Morishita[1], T. Nagira[3], M. Yoshiya[3], K. Uesugi[4], A. Takeuch[4]

[1]Kyoto University, Sakyo, Kyoto, 606-8501, Japan

[2]Osaka Sangyo University, Osaka, 574-0013, Japan

[3]Osaka University, Suita, Osaka, 565-0871, Japan

[4]JASRI/SPring-8, Sayo-cho, Hyogo, 679-5148, Japan

[a]yasuda.hideyuki.6s@kyoto-u.ac.jp

Keywords: ductile cast iron, X-ray, solidification, spheroidal graphite, oxygen potential

Abstract. Time-resolved and in-situ observations using synchrotron radiation X-rays were performed to observe solidification of cast iron (CE=4.5, 0.02mass%Mg). Morphology of graphite particles was influenced by specimen holder material. In the Al_2O_3 holder, graphite particles were spheroidal at the beginning and then deviated from the spheroidal shape. In addition, the coupled eutectic solidification of austenite and graphite occurred at the final stage. In contrast, the divorced eutectic solidification, in which graphite particles and austenite dendrites independently grew, was selected until the end of solidification in MgO holder. Spheroidal graphite particles were engulfed by austenite. Consequently, typical microstructure observed in ductile cast iron was reproduced in the in-situ observation. The results suggested that oxygen potential, which was determined by Al_2O_3 or MgO (specimen holder) in the observations, could be an important factor for the selection of eutectic growth mode and graphite morphology.

Introduction

It is known that small addition of Ce or Mg to cast iron changed the graphite morphology from a flake shape to a more compacted or spheroidal shape [1, 2]. The solidification sequence in the ductile cast iron is rather complicated [3, 4]. The divorced eutectic growth is normally selected in the melt which contains sufficient Mg or Ce, leading to spheroidal or compacted graphite particles in the matrix. It has been proposed that inclusions [5-10] or bubbles [11-13] act as nucleation sites for graphite and contribute to formation of spheroidal shape. In addition, S solved in the melt can degradation graphite shape [14]. However, it is still not clear how the spheroidal graphite particles form during solidification.

Time-resolved and in-situ observations using synchrotron radiation X-rays has allowed to observe solidification in cast iron in-situ [15-18]. The specimens (3.79C - 3.1Si - 0.14Mn - 0.015S - 0.04Mg in mass%, CE=4.8) were repeatedly melted and solidified. In the first run, the graphite particles with spherical shape grew in the melt and were surrounded by austenite dendrites or the coupled eutectic front of austenite and graphite [16, 18]. In the second run and further runs, graphite particles transformed from spheroidal shape to flake-like shape before being engulfed by austenite dendrites or the coupled eutectic front. It was also emphasized that the temperature range in which the graphite particles grew as the primary phase increased with decreasing Mg concentration [17, 18]. It indicates that Mg in the melt can change phase equilibrium between liquid, austenite and graphite. In the previous studies, the coupled eutectic solidification, which is not observed in the ductile cast iron, always occurred at the final stage of solidification. This paper presents influence of specimen holder (Al_2O_3 and MgO) on the microstructure evolution in the hypereutectic cast iron and demonstrates the selection of the divorced eutectic and the formation of spheroidal graphite particles.

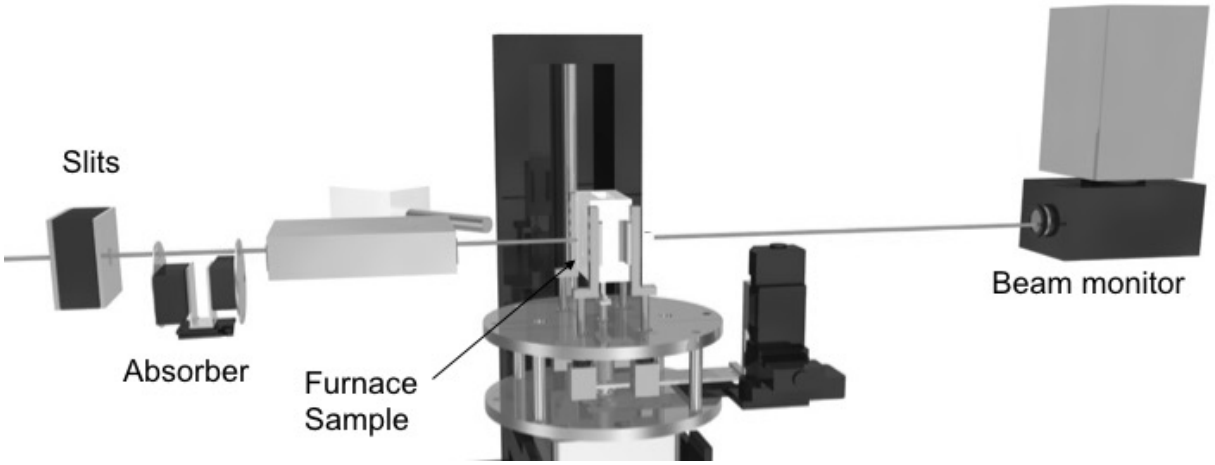

Figure 1 Setup for time-resolved and in-situ observation [15,18].

Experiments

The chemical compositions of specimen is 3.67C-2.63Si-0.45Mn-0.02Mg-0.003S in mass% (CE=4.5). Time-resolved and in-situ observations were performed at BL20XU beamline in SPring-8 (Synchrotron radiation facility in Japan). The X-ray energy used for the observations was 19keV. Figure 1 shows a setup for the in-situ observation. A furnace using a graphite heater, a thin specimen (100 μm in thickness) in a holder (Al_2O_3 and MgO) and an X-ray imaging detector (consisting of a CMOS-type camera, an optical lens and a phosphor screen) were placed along the light axis. Details of the setup were described in previous studies [15, 18]. The transmission image signal was converted into a digital format and stored with a format of 2000 x 1312 pixels and 16-bit resolution. The pixel size was 0.5μm x 0.5μm. For the observation of solidification, the specimen with the microstructure of ductile cast iron was melted and then the melt was cooled at a cooling rate of 0.5K/s under a vacuum atmosphere (in the order of 10^0 Pa).

Results and Discussion

Figure 2 shows a snapshot of solidification in a specimen (Al_2O_3 holder). Despite of the hypereutectic composition (CE=4.5), dendritic growth of austenite and nucleation or growth of graphite particles simultaneously occurred at the beginning of solidification. Namely, the divorced eutectic solidification was selected at the beginning. According to the previous studies [16-18], addition of Mg shifted the eutectic composition to higher carbon concentration. The simultaneous nucleation and growth is explained by considering the shift of eutectic composition.

As shown in the bottom part of Fig.2, the coupled eutectic, in which austenite and lamellar graphite grew side by side, occurred after the divorced eutectic solidification. Since the lamellar spacing was smaller than the thickness of specimen, the coupled eutectic structure caused the foggy contrast on the transmission images (“γ+Gr” in the figure). Since the growth velocity of coupled eutectic was relatively high, the graphite particles and the austenite dendrites were engulfed by the coupled eutectic front within 2-3s.

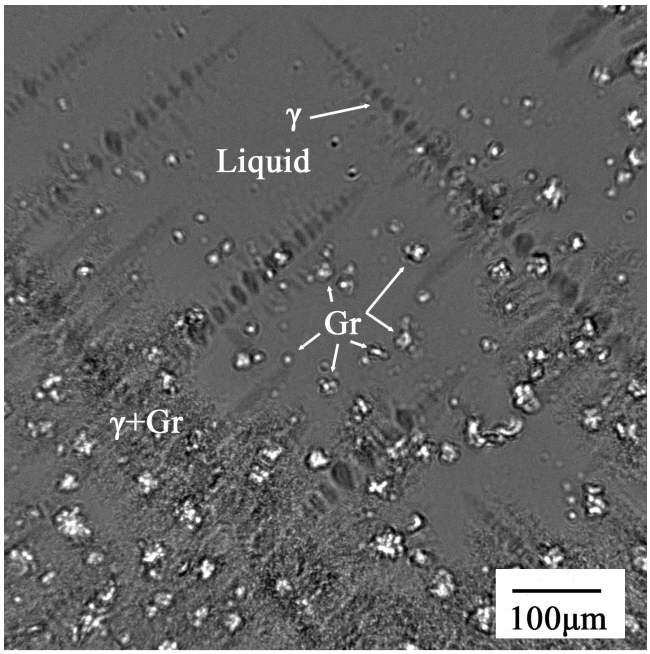

Figure 2 Snapshot of time-resolved and in-situ observation for the spcimen in Al_2O_3 holder. White: Graphite and dark gray: austenite and foggy contrast: coupled eutectic of austenite and graphite.

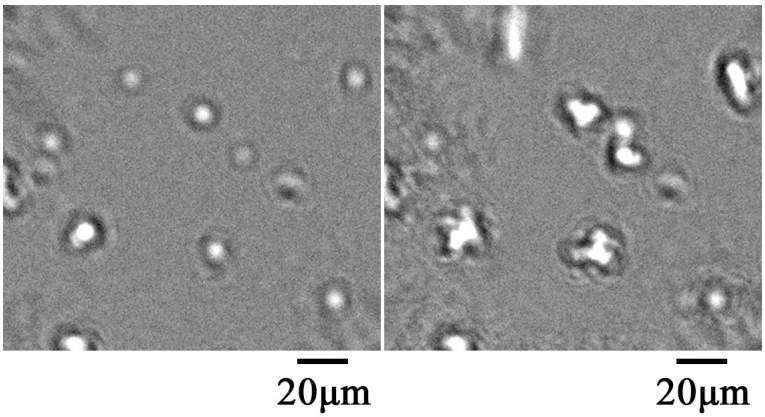

Figure 3 Shape evolution of graphite particles in the specimen (Al_2O_3 holder). Interval between frames is 1s. Floating of graphite particles due to bouyancy force was observed. White: Graphite and dark gray: liquid phase.

Shape evolution of graphite particles in the specimen (Al_2O_3 holder) is shown in Fig.3. The graphite particles were spheroidal at the beginning of growth (just after nucleation in the melt). Deviation from spheroidal shape to rather compacted shape (short branches grew from the spheroidal core) occurred in the melt and consequently circularity was degraded. The degradation of circularity in the melt suggested that the austenite dendrites did not directly influence the graphite growth. It should be noted that the occurrence of the coupled eutectic solidification and the degradation of spheroidal shape before being engulfed differed from the solidification of the ductile cast iron.

Figure 4 shows snapshots of solidification in a specimen (MgO holder). Austenite dendrites grew and simultaneously graphite particles nucleated around austenite dendrites. However, the interaction between the austenite dendritic growth and graphite nucleation was not identified in the observation. Floating of graphite particles showed that the nucleation events occurred in the melt and most of the graphite particles kept spheroidal shape. The engulfment of graphite particles into the austenite occurred when the floating graphite particles touched the austenite dendrite arms. Only the divorced eutectic was selected when the specimen was put in the MgO holder. The microstructure of the specimen in MgO holder essentially agreed with the typical microstructure of the ductile cast iron.

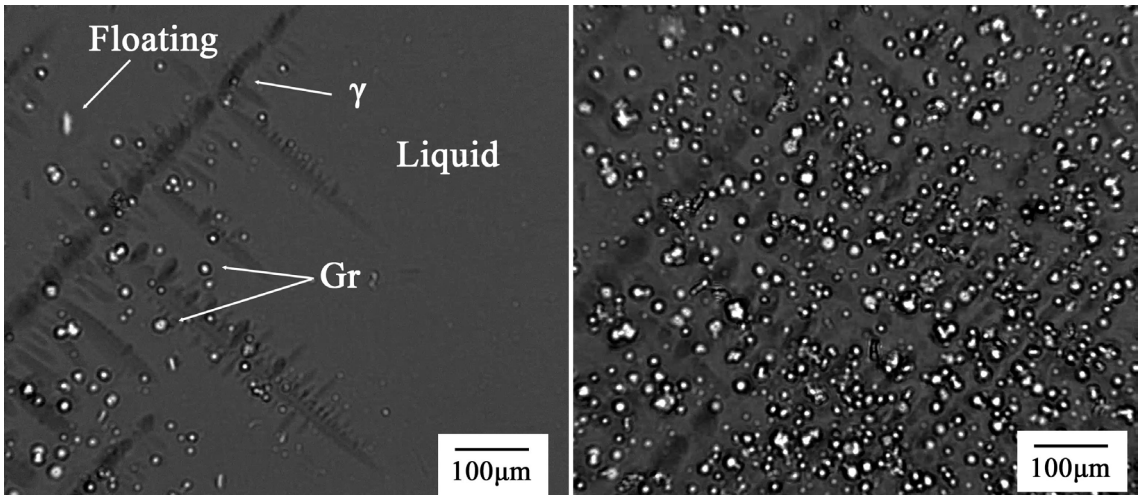

Figure 4 Snapshots of time-resolved and in-situ observation for the specimen in MgO holder. Interval between (a) and (b) is 1s. Floating of graphite particles due to bouyancy force was observed. White: Graphite and dark gray: austenite.

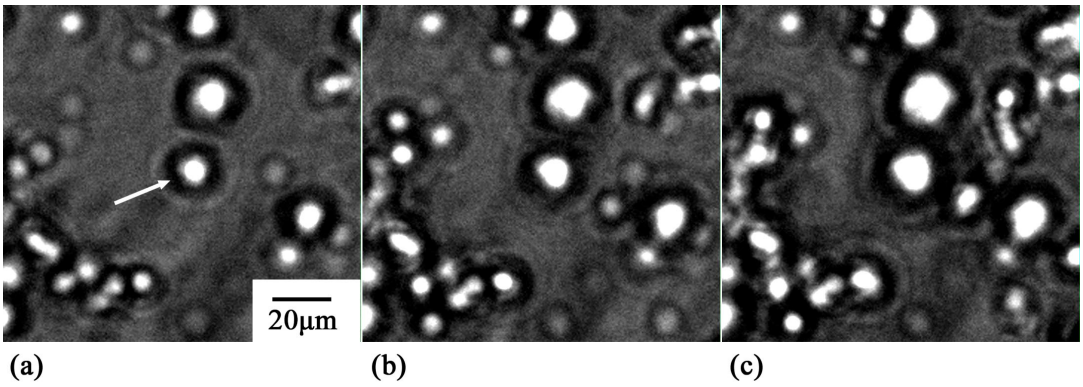

Figure 5 Close-up view of spheroidal graphite particles in the specien (MgO). Graphite particle (a) before engulfed by the austenite, (b) after engulfed by the austenite and (c) at the final stage of solidification. Interval between frames is 7s.

Time evolution of graphite particles in the specimen (MgO holder) is also shown in Fig. 5. The graphite particles indicated by an arrow nucleated and grew in the melt as shown in Fig.5(a), because the most particles moved upward due to the buoyancy force. Figure 5(b) shows spheroidal graphite particles just after the engulfment. The diameter of spheroidal graphite particles in Fig.5(c) is larger than that in Fig.5(b). The observation clearly proved that the spheroidal graphite particles continued to grow in the austenite.

Solidification sequence including selection of eutectic mode and shape evolution of graphite particles were significantly influenced by the specimen holder (Al_2O_3 and MgO). According to the previous studies [5-10], Mg-O-S inclusions were found in the core of spheroidal graphite particles. The role of inclusions as nucleation site is closely related to the spheroidal graphite formation. Possible explanation to the influence of Al_2O_3 and MgO holders on the graphite morphology is that the holder changes concentration of Mg dissolved in the melt and modified inclusions containing Mg in the melt. Oxygen potential is relatively high in the Al_2O_3 holder, comparing to that in the MgO holder. In the Al_2O_3 holder, Mg atoms and MgS / Mg-O-S inclusions in the melt can react with Al_2O_3 (O atoms in the melt). As a result, Mg concentration in the melt decreases and S concentration increases. The concentration changes of Mg and S in the melt and the modification of inclusions can lead to the selection of the coupled eutectic solidification and the shape transformation from spheroidal shape to compacted and flake-like shapes.

Summary

The time-resolved and in-situ observations allowed to observe the evolution of spheroidal graphite particles and shape transformation from spheroidal shape to compacted and flake-like shape.

(1) In the Al_2O_3 holder, the spheroidal graphite particles were formed and then shape evolution from spheroidal to compacted and flake-like occurred before the engulfment. In addition, the coupled eutectic solidification occurred at the final stage of solidification.

(2) In the MgO holder, the graphite particles kept spheroidal shape and were engulfed by the austenite. Only the divorced eutectic solidification was selected until the end of solidification. As a result, the typical microstructure observed in the ductile cast iron was reproduced in the in-situ observation.

(3) The graphite particles nucleated in the melt and continued to grow even in the austenite.

(4) Oxygen potential, which is determined by the holder, significantly influenced the formation of spheroidal graphite particles. The results suggested that Mg disolved in the melt and Mg-O-S inclusions influenced the formation of spheroidal graphite particles. The results will help further understanding for the microstructure evolution in the ductile cast iron.

Acknowledgements

This study was supported by a Grant-in-Aid for Scientific Research (S) from MEXT. The synchrotron radiation experiments were performed as general projects at beamlines of BL20XU and BL20B2 at SPring-8 (JASRI).

References

[1] H. Morrogh, J. W. Grant : J. Iron and Steel Inst., vol. 155 (1947), p.321.

[2] A. P. Gagnebin, K. D. Millis and N. B. Pilling: The Iron Age, Feb. 1949, p.77.

[3] D. M. Stefanescu: Metall. Mater. Trans. A, vol. 38A (2007), p.1433-1447.

[4] H. Zhao, M. Zhu, D. M. Stefanescu: Key Eng. Mater., vol.457 (2011), p.324-329.

[5] K. M. Muzumdar, J. F. Wallace: AFS Transactions, vol. 80 (1972), p.317-328.

[6] K. M. Muzumdar, J. F. Wallace: AFS Transactions, vol. 81 (1973), p.412-423.

[7] G. X. Sun, C. R. Loper: 1983, AFS Transactions, vol.91, p.639-646.

[8] T. Askaland: Metall. Trans. A, vol.24A (1993), p.2321-2345.

[9] M.H. Jacobs, T. J. Law, D. A. Melford, M. J. Stowell: Met. Technol., vol.1 (1974), p.490-500.

[10] N. Klorca-Isern, J. Tartera, M. Espanol, M. Marsal, G. Bertran, S. Castel: Micron, vol.33 (2002), p.357-364.

[11] H. Itofuji: AFS Transactions, vol.104 (1996), p.79-87.

[12] S. Yamamoto, Y. Kawano, Y. Murakami, B. Chang, R. Ozaki: Metal Science, vol.12 (1978), p.56-60.

[13] M. J. Lalich, J. R. Hitchings: AFS Transactions, vol.84 (1976), p.652-658.

[14] H. Nakae, S. Jung, H. Inoue, H. Shin: 2004, Proc. 66th World Foundry Congress, Istanbul, p.917-928.

[15] A, Sugiyama, H. Yasuda, T. Nagira, M. Yoshiya, K. Uesugi, K. Umetani, I. Ohnaka: J. Japan Foundry Engineering Society, vol.82 (2011), p.131-136.

[16] K. Yamane, H. Yasuda, A. Sugiyama, T. Nagira, M. Yoshiya, K. Uesugi, K. Umetani, C. Ushigome, A. Sato: J. Japan Foundry Engineering Society, vol.85 (2013), p.760-770.

[17] K. Yamane, A. Sugiyama, T. Nagira, M. Yoshiya, H. Yasuda, Y. Tanaka, A, Sato, K. Uesugi, A. Takeuchi, Y. Suzuki, H. Honda, K. Sato: J. Japan Foundry Engineering Society, vol.86 (2014), p.461-470.

[18] K. Yamane, H. Yasuda, A. Sugiyama, T. Nagira, M. Yoshiya, K. Morishita, K. Uesugi, A. Takeuchi, Y. Suzuki: Metall. Mater. Trans. A, vol.46A (2015), p.4937-4946.